Regulation of Matrix Metalloproteinase-9 by Epigenetic Modifications and the Development of Diabetic Retinopathy

Qing Zhong and Renu A. Kowluru

Diabetes activates retinal matrix metalloproteinase-9 (MMP-9), and MMP-9 damages the mitochondria and augments capillary cell apoptosis. Our aim is to elucidate the mechanism responsible for MMP-9 activation. Histone modifications and recruitment of the nuclear transcriptional factor-κB (p65 subunit) at the *MMP-9* promoter and the activity of lysine-specific demethylase 1 (LSD1) were measured in the retina from streptozotocin-induced diabetic rats. The role of LSD1 in MMP-9 activation was investigated in isolated retinal endothelial cells transfected with *LSD1* small interfering RNA (siRNA). The results were confirmed in the retina from human donors with diabetic retinopathy. Diabetes decreased histone H3 dimethyl lysine 9 (H3K9me2) and increased acetyl H3K9 (Ac-H3K9) and p65 at the retinal *MMP-9* promoter. LSD1 enzyme activity and its transcripts were elevated. *LSD1* siRNA ameliorated the glucose-induced decrease in H3K9me2 and increase in p65 at the *MMP-9* promoter, and prevented MMP-9 activation, mitochondrial damage, and cell apoptosis. Human donors with diabetic retinopathy had similar epigenetic changes at the *MMP-9* promoter. Thus, activated LSD1 hypomethylates H3K9 at the *MMP-9* promoter and this frees up that lysine 9 for acetylation. Increased Ac-H3K9 facilitates the recruitment of p65, resulting in MMP-9 activation and mitochondrial damage. Thus, the regulation of LSD1 by molecular or pharmacological means has the potential to retard the development of diabetic retinopathy. ***Diabetes* 62:2559–2568, 2013**

Mitochondrial dysfunction is considered as one of the mechanisms responsible for the development of diabetic retinopathy, possibly by initiating the loss of retinal capillary cells, a phenomenon that precedes the development of histopathology (1–3). Increased matrix metalloproteinases (MMPs), especially MMP-2 and MMP-9, are observed in the retina of patients with diabetic retinopathy and in diabetic rodents (4–6), and activated MMPs (2 and 9) damage retinal mitochondria and accelerate cell apoptosis (5–8). *MMP-9* gene transcripts are increased in the retina in diabetes (5,6,9,10), and the retinal vasculature of diabetic mice lacking the *MMP-9* gene shows normal mitochondrial ultrastructure. The vasculature is also protected from the increased apoptosis and histopathology associated with diabetic retinopathy (5). However, the mechanism responsible for the regulation of retinal *MMP-9* transcripts is not clear.

Transcription of genes is controlled by protein complexes, including chromatin-remodeling and transcription factors. Acetylation of histone lysine activates gene transcription (11), and a decrease in general histone acetylation in liver fibrosis and human sarcoma cells is implicated in subnormal *MMP-9* promoter activity (12,13). Unlike acetylation, lysine residues can be mono-, di-, and trimethylated (me1, me2, and me3, respectively). Methylation of lysine 9 of histone 3 (H3K9) is associated with repressive chromatin conformation, but that of lysine 4 of H3 (H3K4) is associated with an open chromatin structure and active transcription (11,14). How histone modifications activate retinal MMP-9 in diabetes needs further investigation.

Demethylation of histones is regulated by a dynamic enzyme, lysine-specific demethylase 1 (LSD1), and demethylation of methyl H3K4 results in gene repression and that of methyl H3K9 in gene activation (15–17). In diabetes, LSD1 reduces methylation of H3K9 at the promoter of the p65 subunit of *NF-κB* (p65), and this is associated with the persistent activation of nuclear transcriptional κB, NF-κB (14). The effect of diabetes on retinal LSD1 and the role of LSD1-mediated demethylation in the activation of retinal MMP-9 remain to be explored.

Transcription of *MMP-9* is controlled by 670 bases of upstream sequence that includes binding sites for transcriptional factors including AP-1, NF-κB, and SP1, and deletion or mutation in any of these binding sites decreases *MMP-9* promoter activity (18,19). Induction of *MMP-9* through activation of NF-κB is considered key for many signaling pathways, and the classic pathway of p65/p50 and alternative pathway p52/RelB can bind to the NF-κB binding site to activate the *MMP-9* promoter (20,21). In the development of diabetic retinopathy, activation of retinal NF-κB is considered proapoptotic (22,23), and the binding of p65 is increased at the promoter and enhancer regions of *Sod2*, the gene that encodes MnSOD (24). The effect of diabetes on the regulation of the *MMP-9* promoter by NF-κB remains unclear.

The aim of this study is to elucidate the mechanism responsible for the regulation of the retinal *MMP-9* promoter in diabetes. Using retina from diabetic rats, we investigated histone methylation at the retinal *MMP-9* promoter and the role of LSD1 in regulating methylation. In addition, the recruitment of *p65* at the *MMP-9* promoter was evaluated. The results were confirmed in retinal endothelial cells, the cells that are the target of the histopathology characteristic of diabetic retinopathy, by genetically modulating LSD1 or NF-κB. To transit from the animal models and in vitro studies to the human disease, the key findings were investigated in the retina from human donors with diabetic retinopathy.

RESEARCH DESIGN AND METHODS

Rats. Six months after streptozotocin-induced diabetes in male Wistar rats (glycated hemoglobin 12.3 ± 2.0%), the retina was removed immediately. One retina was cross-linked with 1% paraformaldehyde for chromatin

From the Kresge Eye Institute, Wayne State University, Detroit, Michigan.
Corresponding author: Renu A. Kowluru, rkowluru@med.wayne.edu.
Received 23 August 2012 and accepted 12 February 2013.
DOI: 10.2337/db12-1141

immunoprecipitation (ChIP), and the other was stored in liquid nitrogen for future analysis. Age-matched normal rats (glycated hemoglobin 5.9 ± 0.9%) served as control.

Mice. Mice overexpressing *Sod2* (MnSOD-Tg) and their wild-type (WT) littermates (~8 weeks of age) or C57BL/6J (control) or *MMP-9* gene knockout (MMP-KO, B6.FVB [Cg]-MMP-9tm1Tvu/J; The Jackson Laboratory, Bar Harbor, ME) were made diabetic by streptozotocin (2,3,5,7,8,25). MnSOD-Tg mice were originally generated in the C3H background, and the hemizygous mice were then bred with WT B6C3 F1 mice to generate MnSOD-Tg mice (26). To avoid any *rd1*-related retinal complications coming from the C3H strain, mice were bred for seven to eight generations with C57BL/6 mice, and the absence of *rd1* was confirmed by genotyping for *rd1*. As previously reported by us, nondiabetic WT and MnSOD-Tg mice had a similar number of degenerative retinal capillaries (2), and nondiabetic and diabetic MMP-KO mice had a similar retinal MMP-9 activity (5,6). The mice were killed after 7–12 months of diabetes by an overdose of pentobarbital, and the retina was isolated under a dissecting microscope.

Treatment of animals followed the National Institutes of Health principles of laboratory animal care and the Association for Research in Vision and Ophthalmology resolution on the use of animals in research guidelines.

Retinal endothelial cells. Bovine retinal endothelial cells (BRECs) from fourth to fifth passage were transfected with *LSD1* small interfering RNA (siRNA) or *p65* siRNA (Santa Cruz Biotechnology, Santa Cruz, CA) as routinely performed in our laboratory (5,24). Parallel incubations were carried out using nontargeting scrambled RNA. At the end of the transfection, the cells were rinsed with PBS and incubated in 5 or 20 mmol/L glucose for 4 additional days. BRECs incubated in 20 mmol/L mannitol served as an osmotic control. Transfection efficiency was determined by quantifying the gene transcripts of *LSD1* or *p65* by semiquantitative PCR and confirmed by real-time quantitative PCR (qPCR).

Human retina. The retina was isolated from human postmortem eyes (Midwest Eye Banks, Ann Arbor, MI). Diabetic donors with an average duration of diabetes of 10–30 years had clinically documented proliferative retinopathy. Age-matched nondiabetic donors served as controls (Table 1). The eyes were enucleated between 6 and 9 h after death and transported on ice. One-third of the retina was selected randomly and fixed in paraformaldehyde, and the rest of the retina was frozen for further analysis. Our previous work has shown that the retina prepared from such postmortem eyes present similar diabetes-induced alterations in the gene expressions as observed in the fresh retina from diabetic rodents (3,6). Furthermore, others have shown stable transcripts in the postmortem samples that are not influenced by the delay (7–24 h) in processing the tissue (27,28).

Gene expression was quantified by SYBR green–based qPCR using the 7500 Real-Time PCR System (Applied Biosystem). Amplification was performed in ~5 ng of ChIP-purified DNA or cDNA using the primers provided in Table 2. The PCR conditions included denaturation at 95°C for 10 min, followed by 40 cycles of denaturation at 95°C for 15 s and annealing and extension at 60°C for 60 s. This was followed with dissociation at 95°C for 15 s, 60°C for 60 s, 95°C for 15 s, and 60°C for 15 s. The specific products were confirmed by SYBR green single melting curve and a single correct-size product on a 1.2% agarose gel. Each sample was measured in duplicate. Values obtained from the immunoprecipitate were normalized to the cycle threshold (Ct) value from the input sample, and those from cDNA were normalized to the Ct value from *β-actin* in the same sample using the delta-delta cycle threshold (ddCt) method. Relative fold changes were calculated by setting the mean fraction of normal rats or cells incubated in 5 mmol/L glucose as 1 (6,24). Taqman primers were used to quantify *MMP-9* gene expression in the rat retina and *LSD1* in BRECs with *β-actin* or *18S* rRNA, respectively, as their housekeeping genes (24). *LSD1* expression was also confirmed by semiquantitative PCR.

Western blotting. Proteins were separated on a 4–20% gradient polyacrylamide gel using primary antibody against the protein of interest and β-actin as the loading control. The band intensity was quantified using UnScan-It Gel digitizing software (Silk Scientific, Orem, UT).

ChIP was performed using a ChIP assay kit (Millipore Corp., Temecula, CA) according to the methods used in our laboratory (24,25). Protein-DNA complex (100–120 μg) was immunoprecipitated with the antibody against H3K4me1, H3K4me2, H3K9me2, LSD1, acetyl H3K9, p65, or general transcription factor IIB (TFIIB). DNA fragments were recovered by phenol:chroloform:isoamyl alcohol extraction, followed by ethanol precipitation, and resuspended in 14 μL water for PCR. *MMP-9* promoter was quantified in the extracted DNA (~5 ng) by SYBR green–based qPCR. Normal rabbit IgG was used as a negative antibody control and DNA from the input (20–40 μg protein-DNA complex) as an internal control. Each ChIP measurement was made with five to six samples per group. *MMP-9* promoter precipitated by H3K4me2, p65, or normal rabbit IgG was confirmed by semiquantitative PCR, and the conditions included denaturation at 95°C for 2 min, 30 cycles of denaturation at 92°C for 45 s, annealing at 60°C for 1 min, and extension at 72°C for 45 s. Specificity of the ChIP assay was verified by semiquantitative PCR; the off-target region of rat *MMP-9* (nonpromoter region, +1859 to +2232) occupied by H3K4me2 was amplified for negative target control, and rat *β-actin* promoter bound by TFIIB served as a positive control. Whereas the promoter sequence of the *MMP-9* gene (−650 to +1 bp upstream) is ~70% homologous among human, rat, cow, and mouse, the NF-κB binding site sequence is 90–100% conserved among these species (18).

LSD1 activity was quantified in the retina using the LSD1 Fluorescent Assay kit (BPS Bioscience, San Diego, CA) according to the manufacturer's instructions. Nuclear protein (5 μg), isolated by the Nuclear Extract kit (Active Motif, Carlsbad, CA), was incubated at room temperature for 30 min with 2× assay buffer and methyl peptide. The reaction mixture was then incubated for 5 min with Amplex red and peroxidase, and H_2O_2 production was quantified at 540-nm excitation and 600-nm emission wavelengths.

TABLE 1
Human donors

	Age (years)	Duration of diabetes (years)	Cause of death	Laser therapy
Nondiabetic donors				
1	44	—	Intracranial hemorrhage	
2	37	—	Asthma	
3	70	—	Myocardial infarction	
4	72	—	Myocardial infarction	
5	55	—	Subarachnoid hemorrhage	
6	77	—	Myocardial infarction	
7	57	—	Myocardial infarction	
8	70	—	Cerebrovascular accident	
Donors with diabetic retinopathy				
1	75	25	Pulmonary edema	+
2	66	30	Acute myocardial infarction	+
3	54	10	Unknown	
4	61	10	Acute myocardial infarction	+
5	68	10	Congestive heart failure	+
6	59	25	Pneumonia	+
7	47	27	Acute myocardial infarction	+
8	75	30	Acute myocardial infarction	+
9	68	10	Congestive heart failure	+

+, Patients who received laser therapy.

TABLE 2
Primer sequence

Gene	Primer sequence	Position
Rat		
MMP-9 promoter		
Forward	TGCCCCTGAGGCTTCCCCAA	−644 to −625
Reverse	TGGAGCCCCTCCCCACACTG	−466 to −485
β-actin promoter		
Forward	ACGGAACCAGCACCCATCGC	−267 to −248
Reverse	CGCGGACTCGACAGTGGCTG	+12 to −9
MMP-9 off-target		
Forward	ATGGTGCCCCATGTCACTTT	1859 to 1878
Reverse	GAATGGAAATACGCAGGGTTTG	2232 to 2211
LSD1		
Forward	ACGCAAGCGGGCGAAGGTAG	480 to 499
Reverse	ACGGCTCCTCGGGCTCACTT	658 to 639
β-actin		
Forward	CCTCTATGCCAACACAGTGC	957 to 976
Reverse	CATCGTACTCCTGCTTGCTG	1171 to 1152
Bovine		
MMP-9 promoter		
Forward	CAGACGCCACAACACTCCCA	−719 to −700
Reverse	TCCTCTCCCTGCTCCACCTG	−546 to −565
MMP-9		
Forward	CTGGAGGTTCGACGTGAAGAC	1917 to 1937
Reverse	AAGGTCACGTAGCCCACATAGTC	2117 to 2095
LSD1		
Forward	GTTGGCCGATGCCTGGCCAT	2369 to 2388
Reverse	CCAGGGATCAGCACGCCAGC	2467 to 2448
β-actin		
Forward	CGCCATGGATGATGATATTGC	89 to 109
Reverse	AAGCCGGCCTTGCACAT	154 to 138
Human		
MMP-9 promoter		
Forward	GATTCAGCCTGCGGAAGACAGGG	−638 to −616
Reverse	CCAAACCCCTCCCCACACTCCA	−471 to −492
MMP-9		
Forward	CACTGTCCACCCCTCAGAGC	1438 to 1457
Reverse	GCCACTTGTCGGCGATAAGG	1700 to 1681
LSD1		
Forward	GCAGCCACCAGCCGTTCAGT	2117 to 2136
Reverse	TCACCCCTGCTGGCAGTCGT	2290 to 2271
β-actin		
Forward	AGCCTCGCCTTTGCCGATCCG	34 to 54
Reverse	TCTCTTGCTCTGGGCCTCGTCG	270 to 249
Mouse		
MMP-9		
Forward	CAGAGCGTCATTCGCGTGGA	1993 to 2012
Reverse	AAGGGCACTGCAGGAGGTCGTA	2197 to 2176
LSD1		
Forward	CGCAAGCGGGCCAAGGTAGA	478 to 497
Reverse	ACCAGACGGCTCTTCCGGCT	660 to 641
β-actin		
Forward	CCTCTATGCCAACACAGTGC	955 to 974
Reverse	CATCGTACTCCTGCTTGCTG	1169 to 1150

LSD1 activity in BRECs was quantified by chemiluminescent assay (BPS Bioscience). Nuclear protein (5–10 μg) was incubated for 1 h with 1× assay buffer on a methylated histone H3–coated plate. The formation of demethylated H3 was captured by a specific antibody and developed using horseradish peroxidase–labeled secondary antibody.

MMP-9 activity was measured by in situ zymography (5,6). In brief, conditioned medium (15–30 μL) was mixed with 4× zymograph sample buffer and electrophoresed on 8% SDS-polyacrylamide gel containing 1 mg/mL gelatin. The gel was washed with 2.5% Triton X-100, developed using 1× developing buffer (Bio-Rad, Hercules, CA), and stained with 2% (vol/vol) Coomassie blue G-250 (Sigma-Aldrich, St. Louis, MO). The intensity of the active band of MMP-9 (82–86 kDa) was quantified using Un-Scan-It Gel digitizing software.

Caspase-3 activity was measured using a kit from Enzo Life Sciences (Farmingdale, NY) as reported previously (29). In brief, 20–25 μg of retinal homogenate was incubated with Ac-DEVD-*p*-nitroaniline, and the formation of *p*-nitroaniline was quantified spectrophotometrically at 405 nm.

Apoptosis of retinal endothelial cells was determined by ELISA using Cell Death Detection ELISA^{PLUS} as routinely performed in our laboratory (1,29).

Reactive oxygen species. The cells were incubated for 45 min with 10 μmol/L of 2',7'-dichlorofluorescein diacetate (DCDHF; Enzo Life Sciences), washed with PBS, and resuspended in PBS with protease inhibitors. Fluorescence was measured at 485-nm excitation and 516-nm emission wavelengths (30,31).

Mitochondrial morphology was determined by electron microscopy. After incubation of cells (transfected with *LSD1* siRNA or untransfected cells) with

high glucose, they were fixed in 2% glutaraldehyde in 100 mmol/L cacodylate, washed with 7% sucrose, embedded in 2% agar, and incubated in 1% osmium oxide (3,5). They were then dehydrated using graded ethanol solutions and embedded in 812 resin (Electron Microscope Sciences, Hatfield, PA). Ultrathin transverse sections (70–80 nm) were stained with uranyl acetate–lead citrate mixture and imaged under a transmission electron microscope (model 400; Phillips, Eindhoven, the Netherlands).

Statistical analysis. Data are expressed as mean ± SD. Statistical analysis was carried out using SigmaStat software. The Kolmogorov-Smirnov test was used to test for normal distribution of the data. One-way ANOVA followed by Bonferroni test was used for data with normal distribution, and Kruskal-Wallis one-way analysis followed by Dunn test was used for data that did not present normal distribution. $P < 0.05$ was considered statistically significant.

RESULTS

Diabetes epigenetically modifies retinal *MMP-9* promoter. Since demethylation of H3K4 is associated with gene repression and that of H3K9 with activation (11,14–17), we investigated the effect of diabetes on the methylation status of H3K4 and H3K9 at the *MMP-9* promoter. Diabetes increased methylation of H3K4 at the *MMP-9* promoter (Fig. 1*A*), and the levels of H3K4me1 and -me2 were elevated by twofold compared with the values obtained from age-matched normal rat retina. Normal rabbit IgG, used as a negative antibody control, precipitated <10% of the product from ChIP with H3K4me1, -me2, and H3K9me2 antibodies. Increased H3K4me2 at the *MMP-9* promoter was confirmed by semiquantitative PCR, and Fig. 1*B* shows a significant increase in H3K4me2 at the *MMP-9* promoter. In contrast, as a control, IgG antibody produced almost undetectable PCR products at the *MMP-9* promoter. To verify the specific binding at the *MMP-9* promoter and validate the ChIP assay, the binding of H3K4me2 at the off-target region of *MMP-9* was also quantified, and Fig. 1*B* shows almost negligible H3K4me2 at the off-target region of the *MMP-9* promoter. Contrary to this, *β-actin* promoters occupied by TFIIB were strong in both normal and diabetic rat retina (Fig. 1*B*). In the same animals, however, H3K9me2 was decreased by ~45% (Fig. 1*A*). Consistent with our previous results showing increased retinal MMP-9 in diabetes (5,6,10), histone modifications at the *MMP-9* promoter were accompanied by an increase in its gene transcripts (Fig. 1*C*).

To investigate the mechanism responsible for decreased methylation of H3K9, the demethylation enzyme LSD1 was quantified. Figure 2*A* shows that diabetes increased the activity of LSD1 by ~50% and its gene and protein expressions by over twofold compared with the values from age-matched normal rats (Fig. 2*B* and *C*). Consistent with a decrease in H3K9me2 (Fig. 1*A*), an increase in LSD1 was accompanied by its increased recruitment at the *MMP-9* promoter (Fig. 2*D*). To determine if the decrease in H3K9me2 was sufficient to open up the chromatin and facilitate binding of *MMP-9* activators, gene activation markers acetyl H3K9 and p65 were quantified. Contrary to a decrease in H3K9me2 at the *MMP-9* promoter, acetyl H3K9 was increased by almost 18-fold and the recruitment of p65 was elevated by 30-fold (Fig. 2*E*).

Since MMP-9 is regulated by oxidative stress and activated MMP-9 in diabetes damages retinal mitochondria (5,32), to further corroborate the role of increased superoxide in the regulation of MMP-9, the effect of overexpression of MnSOD on LSD1 and MMP-9 was determined. Regulation of mitochondrial superoxide in mice ameliorated the diabetes-induced increase in *LSD1* and *MMP-9* gene

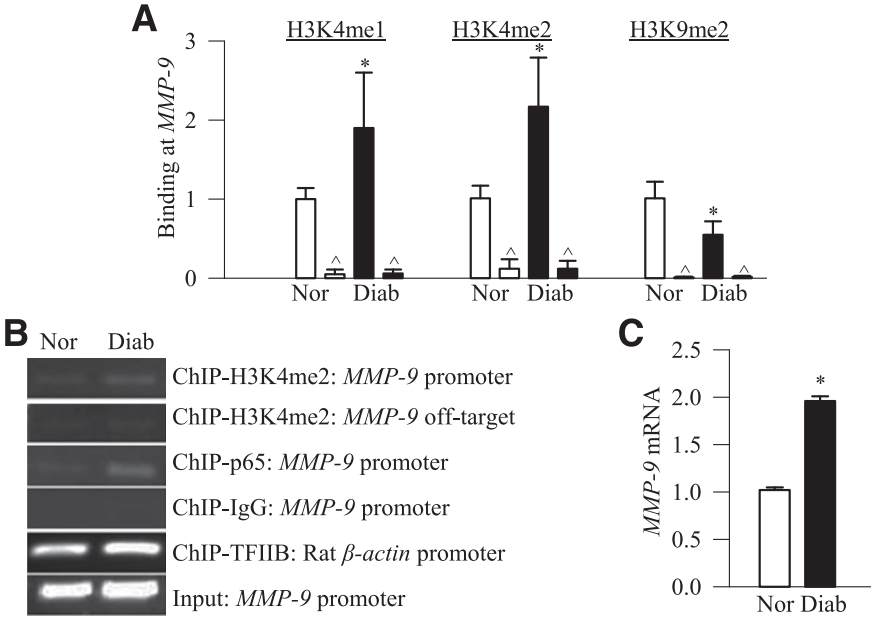

FIG. 1. Methylation of H3K4 and H3K9 at the *MMP-9* promoter is altered in the retina of diabetic rats. *A*: H3K4me1, H3K4me2, and H3K9me2 at the *MMP-9* promoter were determined using ChIP technique followed by SYBR green–based qPCR. Retinal chromatins were immunoprecipitated with antibodies against H3K4me1, H3K4me2, and H3K9me2, and the *MMP-9* promoter region was amplified. The qPCR value in each immunoprecipitate was normalized to the Ct value from the input sample using the ddCt method. Rabbit IgG served as a negative antibody control (indicated as ^). *B*: The specificity of the ChIP assay was verified by semiquantitative PCR. Cross-linked retina was immunoprecipitated with H3K4me2 or p65, and the *MMP-9* promoter occupied by H3K4me2 or p65, respectively, was amplified. DNA from the input (protein-DNA complex) was used as an internal control. For the ChIP assay, the positive controls were *β-actin* promoter occupied by TFIIB, and the negative controls included the *MMP-9* promoter pulled down by normal rabbit IgG as negative antibody control and off-target region of *MMP-9* (+1859 to +2232 bp region) occupied by H3K4me2 as off-target control. *C*: Gene expression of *MMP-9* was quantified by Taqman-based qPCR and analyzed by ddCt method using *β-actin* as the housekeeping gene. Fold changes were calculated by setting the mean fraction of normal rats as 1. Values are represented as mean ± SD of five to seven rats in each group. *$P < 0.05$ compared with normal. Diab, diabetes; Nor, normal.

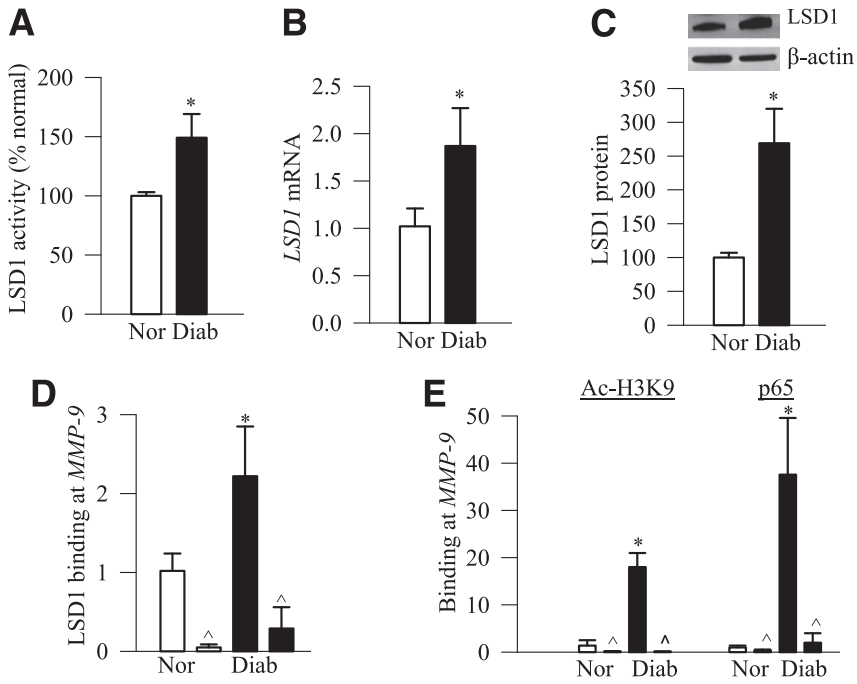

FIG. 2. Diabetes in rats activates retinal LSD1 and increases the recruitment of LSD1 and p65 at the promoter region of *MMP-9*. *A*: Enzyme activity of LSD1 was quantified in rat retinal nuclear fraction using a fluorescent assay kit. After the addition of Amplex red and peroxidase to the reaction mixture, the H_2O_2 produced was measured at 540-nm excitation and 600-nm emission wavelengths. Gene expression of *LSD1* was quantified by qPCR (*B*), and its protein expression was quantified by Western blot technique (*C*). At the *MMP-9* promoter, LSD1 binding (*D*) and acetyl H3K9 (Ac-H3K9) and p65 (*E*) were quantified by the ChIP technique using rabbit IgG as a negative antibody control (marked as ^). Each measurement was made in duplicate in six to seven rats per group. Values obtained from normal rats are considered as 100% or 1 and are presented as mean ± SD. **P* < 0.05, compared with normal. Diab, diabetes; Nor, normal.

transcripts; the values obtained from the retina of MnSOD-Tg diabetic mice were significantly lower compared with those obtained from WT diabetic mice (Fig. 3*A* and *B*). In the same MnSOD-Tg diabetic mice, an increase in retinal MMP-9 protein was also prevented (Fig. 3*C*).

To investigate the effect of *MMP-9* deletion on retinal apoptosis, caspase-3 activity was measured. As expected, caspase-3 activity was increased in the retina from control diabetic mice, which was prevented by the deletion of *MMP-9*; caspase-3 activity in MMP-KO diabetic mice was significantly lower compared with that in control diabetic mice (Fig. 3*D*).

High glucose epigenetically modifies *MMP-9* in retinal endothelial cells. To confirm the role of epigenetic modifications of *MMP-9* in diabetic retinopathy, the effect of high glucose on the methylation status of H3K9 was quantified in BRECs. Glucose decreased H3K9me2 at the *MMP-9* promoter by >70% and increased the recruitment of LSD1 by 1.6-fold compared with the cells exposed to normal glucose (Fig. 4*A* and *B*). Acetyl H3K9 and the recruitment of p65 at the *MMP-9* promoter were also increased by more than twofold (Fig. 4*B*). The specificity of the ChIP assay was validated using IgG antibody control, and the values obtained from the IgG antibody were <10% of the ChIP antibodies. Incubation of BRECs in 20 mmol/L mannitol did not affect H3K9me2 at the *MMP-9* promoter, suggesting that the observed effects of high glucose on histone modifications were not due to an increase in the osmolarity. High glucose also increased LSD1 enzyme activity by 75% and its protein and gene expressions by over twofold compared with the cells incubated in normal glucose (Fig. 5*A*–*C*).

Effect of regulation of LSD1 in retinal endothelial cells on glucose-induced epigenetic changes at the promoter of *MMP-9*. To investigate the effect of inhibition of LSD1 on histone modifications at the *MMP-9* promoter, the BRECs were transfected with *LSD1* siRNA; Fig. 5*D* is included to show the efficiency of transfection. *LSD1* siRNA alleviated the glucose-induced decrease in H3K9me2 and prevented increased recruitment of LSD1 at the *MMP-9* promoter (Fig. 4*A* and *B*). Furthermore, p65 recruitment was also significantly decreased (Fig. 4*B*). In the same *LSD1* siRNA–transfected cells, the glucose-induced increase in LSD1 protein and mRNA was also prevented (Fig. 5*B* and *C*). The values obtained from *LSD1* siRNA–transfected cells in high glucose were significantly different from those obtained from untransfected cells or scramble RNA–transfected cells in high glucose.

To confirm if glucose-induced activation of *MMP-9* is via LSD1, the effect of *LSD1* siRNA on MMP-9 was determined. Transfection of cells with *LSD1* siRNA prevented the glucose-induced increase in *MMP-9* transcripts (Fig. 6*A*) and the activation of MMP-9, as determined by decreased formation of the active form of MMP-9 in the media (Fig. 6*B*). The values obtained from the cells transfected with scramble RNA or untransfected cells incubated in high glucose were significantly higher compared with *LSD1* siRNA–transfected cells. Consistent with our previous results showing similar high glucose–induced activation of MMP-9 in the medium and mitochondria (5), these results strongly suggest that the regulation of *LSD1* may also prevent activation of mitochondrial MMP-9.

To further confirm that LSD1-mediated regulation of *MMP-9* is via p65, the effect of *LSD1* siRNA on p65 was investigated. *LSD1* siRNA prevented the glucose-induced

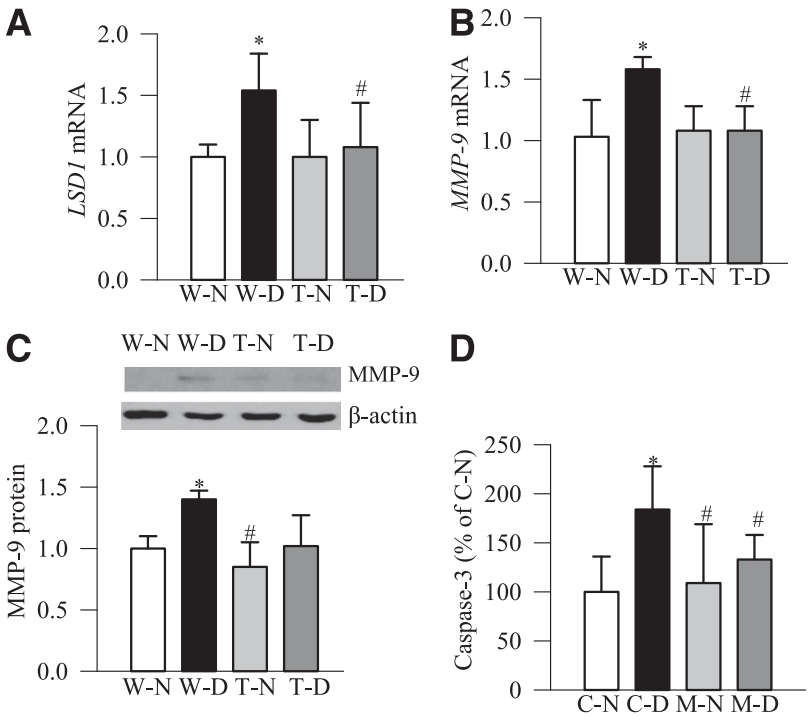

FIG. 3. Diabetic mice overexpressing MnSOD are protected from an increase in retinal LSD1 and MMP-9, and deletion of *MMP-9* prevents diabetes-induced activation of retinal caspase-3. Gene transcripts of *LSD1* (*A*) and *MMP-9* (*B*) were quantified in the retina using TRIzol reagent. Gene expression was measured by SYBR green–based qPCR using ABI-7500 sequence detection system. Each sample was analyzed in triplicate, and the data were normalized to *β-actin* expression. Fold change relative to the age-matched WT normal mice was calculated using the ddCt method. *C*: MMP-9 protein expression was quantified by Western blot technique using β-actin as a loading control; the blot is representative of five to six mice in each group. *D*: Activity of caspase-3 was measured in the retinal homogenate from MMP-KO and control diabetic and nondiabetic mice spectrophotometrically by quantifying the formation of *p*-nitroaniline at 405 nm. Results are from five to eight mice in each group and are represented as mean ± SD. The values obtained from nondiabetic WT or control mice are adjusted to 1 or 100%. W-N and T-N, WT and MnSOD-Tg normal mice; W-D and T-D, WT and MnSOD-Tg diabetic mice; C-N and M-N, control and MMP-KO normal mice; C-D and M-D, control and MMP-KO diabetic mice. *$P < 0.05$, compared with WT-N or C-N; #$P < 0.05$, compared with WT-D or M-D.

increase in p65 binding at the *MMP-9* promoter (Fig. 4*B*) and attenuated the increase in p65 gene and protein expressions (Fig. 6*C*). Furthermore, direct regulation of *p65* by its siRNA also prevented the glucose-induced increase in *MMP-9* transcripts (Fig. 6*A*). The transfection efficiency of *p65* siRNA was 40–50%, and these values were similar to those reported by us previously (24).

The role of LSD1-mediated regulation of MMP-9 in the loss of retinal capillary cells was confirmed by measuring the effect of *LSD1* siRNA on glucose-induced apoptosis; inhibition of *LSD1*, in addition to ameliorating the increase in MMP-9 and NF-κB, also prevented endothelial cell apoptosis (Fig. 6*D*). High glucose–induced values obtained from the untransfected cells or the cells transfected with scramble RNA were about twofold higher than those obtained from cells transfected with *LSD1* siRNA.

To determine if LSD1-mediated regulation of MMP-9 is via mitochondrial superoxide, mitochondrial damage and reactive oxygen species (ROS) levels were quantified. High glucose–induced mitochondrial swelling, partial cristolysis, and increase in ROS were prevented in *LSD1* siRNA–transfected cells (Fig. 6*E* and *F*).

Epigenetic modifications of *MMP-9* in the retina from human donors with diabetic retinopathy. As with the retina from diabetic rats and mice (5,10), *MMP-9* gene transcripts were elevated by ~50% in the donors with diabetic retinopathy, and this was accompanied by similar increases in *LSD1* gene transcripts compared with nondiabetic donors (Fig. 7*A* and *B*). Although H3K9me2 at the *MMP-9* promoter was decreased in diabetic retinopathy donors, the values did not achieve statistical significance (Fig. 7*C*). However, consistent with the results from the rat retina and BRECs, acetyl H3K9 and the recruitment of p65 at the *MMP-9* promoter were elevated by almost twofold compared with age-matched nondiabetic donors, and as a control, normal rabbit IgG yielded <10% of the ChIP antibodies (Fig. 7*C*).

DISCUSSION

In the pathogenesis of diabetic retinopathy, MMP-9 is activated in the retina, and the activation of MMP-9 is considered one of the key events that damages mitochondrial function and structure and activates the apoptotic machinery (5,10,29,33,34). Here we have provided the mechanistic details to show how diabetes activates retinal MMP-9; this is the first report showing that diabetes epigenetically modifies *MMP-9*; H3K9me2 is decreased and acetyl H3K9 and the recruitment of LSD1 and transcription factor NF-κB are increased at the *MMP-9* promoter. *LSD1* silencing in BRECs ameliorates the glucose-induced decrease in H3K9me2 and increase in p65 at the *MMP*-9 promoter, prevents the activation of MMP-9 (transcripts and enzymatic activity), and inhibits cell apoptosis. Furthermore, damage to the mitochondrial ultrastructure and an increase in ROS are also prevented by *LSD1* siRNA, suggesting a close association between LSD1-mediated *MMP-9* epigenetic modifications and oxidative stress. Together, these results strongly imply that the histone modifications of the *MMP-9* promoter, mediated via

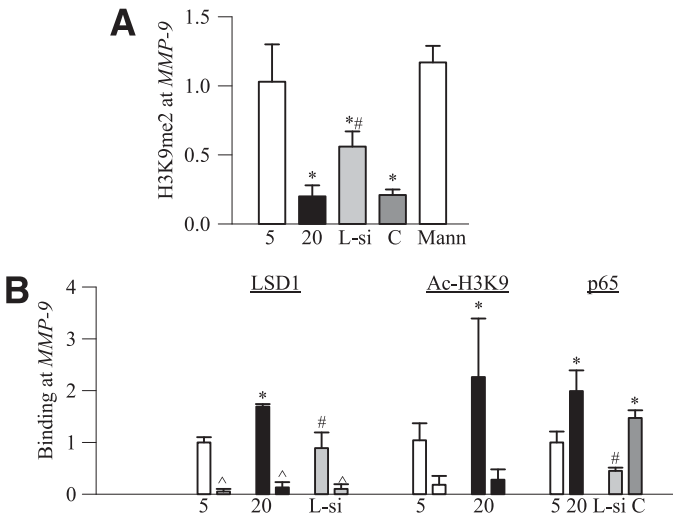

FIG. 4. Lysine 9 of histone 3 is modified and the recruitment of LSD1 and p65 at the *MMP-9* promoter is increased in retinal endothelial cells exposed to high glucose. H3K9me2 (*A*), LSD1, acetyl H3K9, and p65 (*B*) at the promoter region of *MMP-9* were quantified by the ChIP technique. Rabbit IgG was used as negative antibody control (indicated as ^). Fold change relative to the values from cells incubated in 5 mmol/L glucose was calculated by the ddCt method, and the values from 5 mmol/L glucose are considered as 1. Ac-H3K9, acetyl H3K9; IgG, ChIP with normal rabbit IgG; 5 and 20, cells incubated in 5 or 20 mmol/L glucose; L-si and C, cells transfected with *LSD1* siRNA or scramble RNA, respectively, followed by incubation in 20 mmol/L glucose; Mann, cells incubated in 20 mmol/L mannitol. Data are represented as mean ± SD from four to six preparations in each group. *$P < 0.05$, compared with 5 mmol/L glucose; #$P < 0.05$, compared with 20 mmol/L glucose.

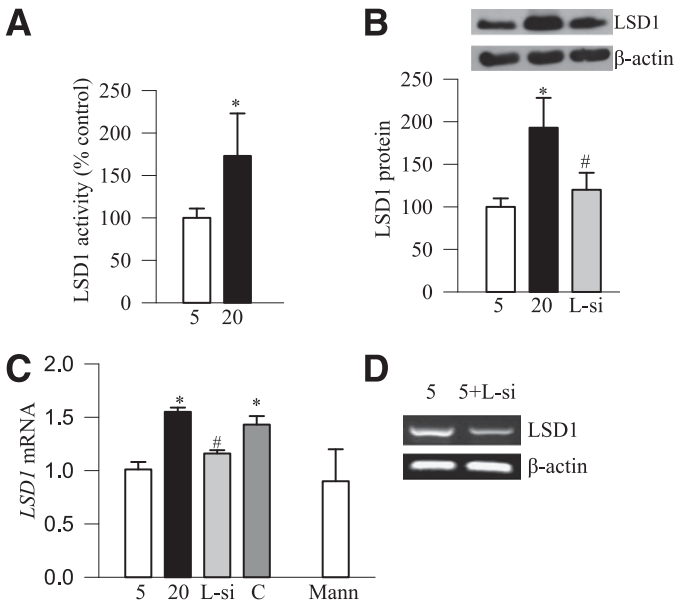

FIG. 5. High glucose exposure of retinal endothelial cells increases LSD1. BRECs were analyzed for LSD1 activity (*A*) in the nuclear fraction by chemiluminescent assay, and the values obtained from control cells incubated in 5 mmol/L glucose are considered as 100%. *B*: Protein expression by Western blot technique using β-actin as a housekeeping protein. *C* and *D*: Gene expression by semiquantitative PCR using *β-actin* as housekeeping gene. 5 and 20, cells incubated in 5 or 20 mmol/L glucose; 5+L-si, cells transfected with *LSD1* siRNA and incubated in 5 mmol/L glucose; L-si and C, cells transfected with *LSD1* siRNA or scramble RNA, respectively, followed by incubation in 20 mmol/L glucose medium; Mann, cells incubated in 20 mmol/L mannitol. Values are mean ± SD from three to five preparations in each group, each measurement made in duplicate, and 5 mmol/L glucose values are considered as control and adjusted to 100% or 1. *$P < 0.05$ and #$P < 0.05$, compared with the values from cells incubated in 5 mmol/L glucose and 20 mmol/L glucose, respectively.

LSD1, are important in the activation of retinal MMP-9 in diabetes.

Histone modifications regulate gene expression by affecting the accessibility of chromatin to the transcription factors. Depending on the site of methylation, histone lysine methylation can signal either activation or repression of the gene. For example, although hypermethylated H3K4 is generally related to gene activation, hypermethylated H3K9 is related to gene repression (11,14). The results presented here show that hyperglycemia elevates H3K4me1 and H3K4me2 at *MMP-9* promoter but decreases H3K9me2. These results are consistent with those reported by others showing an association between hypermethylation of H3K4 and hypomethylation of H3K9 and the transcriptional activation of *MMP-9* in a human cancer cell line (19). Furthermore, in support of our results, hyperglycemia produces similar dynamic cooperativity of histone methylase and demethylases in aortic endothelial cells where hypermethylation of H3K4 and hypomethylation of H3K9 are considered to participate in the activation of NF-κB (14).

Methyl status of histones is regulated by histone-modifying enzymes; histone methyltransferases catalyze the transfer of one, two, or three methyl groups to lysine or arginine residues of histones, and histone demethylases remove methyl groups (35). LSD1 specifically removes the methyl group from mono- and dimethylated H3K4 and H3K9 via a redox process (15–17,36). Removal of methyl groups from H3K4me2 by LSD1 induces transcriptional repression, whereas removal from H3K9me2 results in activation (11,37). Here we show that this demethylating enzyme is activated in hyperglycemic conditions, and increase in LSD1 activity is accompanied by its increased expression, both gene and protein. Furthermore, the recruitment of LSD1 at the *MMP-9* promoter is also increased, suggesting that in addition to demethylation of H3K9me2, this increased recruitment of LSD1 at the promoter region could be contributing to the maintenance of active MMP-9 that the retina experiences in diabetes. The role of LSD1 in MMP-9 activation is further confirmed by our results showing that the regulation of LSD1 by its siRNA prevents a decrease in H3K9me2 and an increase in the recruitment of LSD1.

Gene expression of MMPs is largely regulated at the transcriptional level and *MMP-9* promoter contains *cis*-acting regulatory elements for binding with the transcription factors, including AP-1 (−533 and −79 bp) and NF-κB (−600 bp). Regulation of MMP-9 protein levels has been largely ascribed to transcriptional activation of the gene via binding with these transcription factors (38–40). In accordance with decreased H3K9me2 at retinal *MMP*-9 promoter in diabetes, our results also show that acetyl H3K9 and the recruitment of p65 are also increased. Since hypomethylation and hyperacetylation of H3K9 are associated with the loosening of chromatin, and acetylation of histones alters the folding properties of the chromatin to facilitate the binding surface for the recruitment of other elements (41), these results clearly demonstrate that diabetes-induced modifications at H3K9 help recruit p65 at the *MMP-9* promoter, resulting in the activation of *MMP-9*. To further confirm this, we show that the inhibition of LSD1 by its siRNA prevents increased recruitment of p65 at the *MMP-9* promoter. In support, others have shown LSD1-mediated demethylation of H3K9 at the promoter of

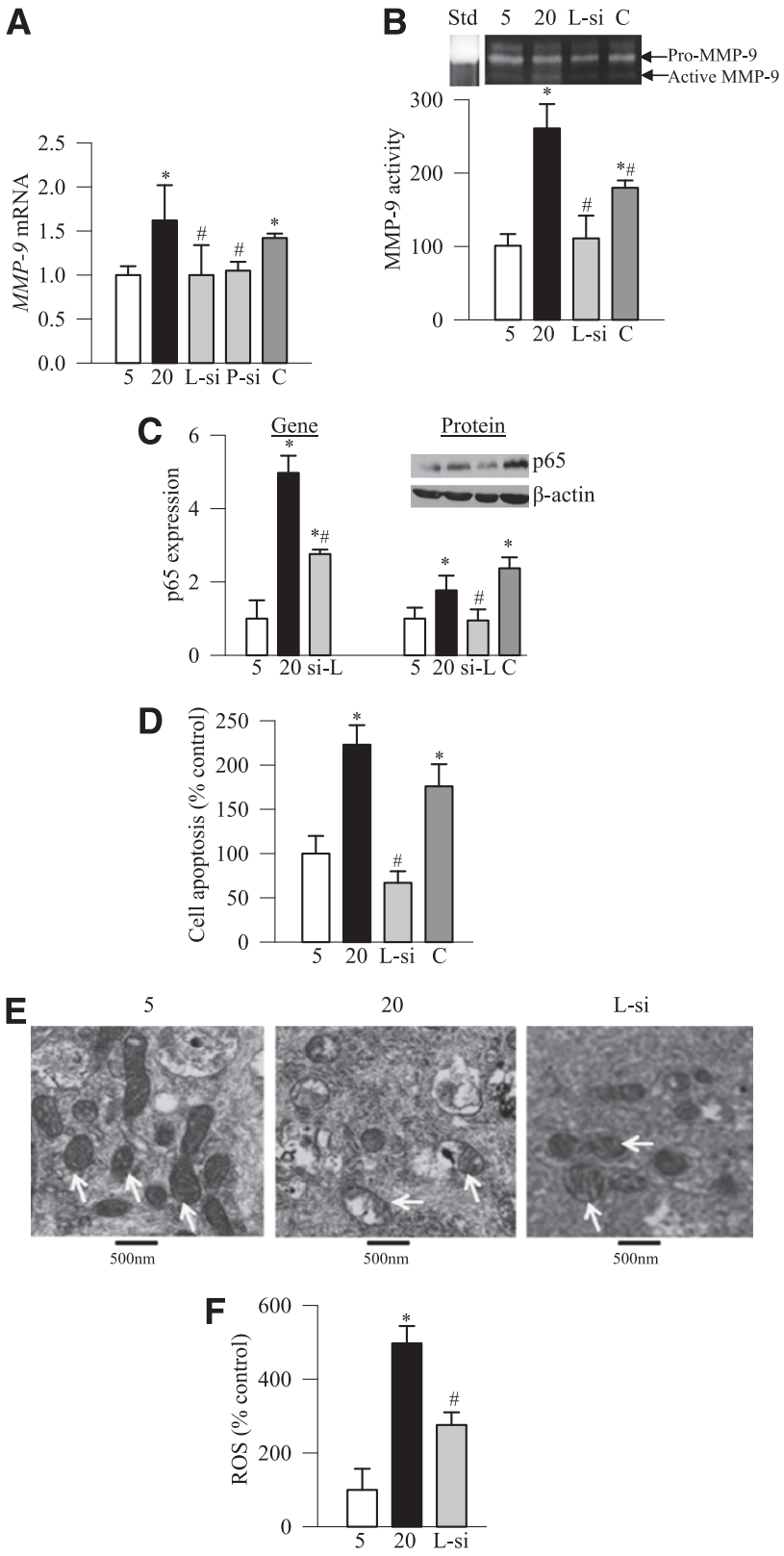

FIG. 6. *LSD1* siRNA of retinal endothelial cells prevents glucose-induced increase in MMP-9, p65, cell apoptosis, and ROS and protects mitochondrial damage. Cells transfected with *LSD1* or *p65* siRNA or scramble RNA were exposed to high glucose for 4 days. *A*: *MMP-9* gene expression was quantified by SYBR green–based qPCR. *B*: MMP-9 activity was measured in the incubation medium by in situ zymography using pro-MMP-9 (human recombinant) as a marker. The active form of MMP-9 (82–86 kDa) relative to the latent form (92 kDa) was quantified and is presented in the accompanying histogram. *C*: Gene expression and protein level of the p65 subunit of NF-κB were quantified by qPCR and Western blot techniques, respectively, using β-actin as an internal control. *D*: Cell apoptosis was measured using an assay kit from Roche Diagnostics. ELISA for cytoplasmic histone-associated DNA fragments was performed. *E*: Morphology of the mitochondria was determined by electron microscopy using ultrathin sections of the cells embedded in 812 resin. Mitochondria were analyzed by ImageJ software in 8–10 images per sample and three to five

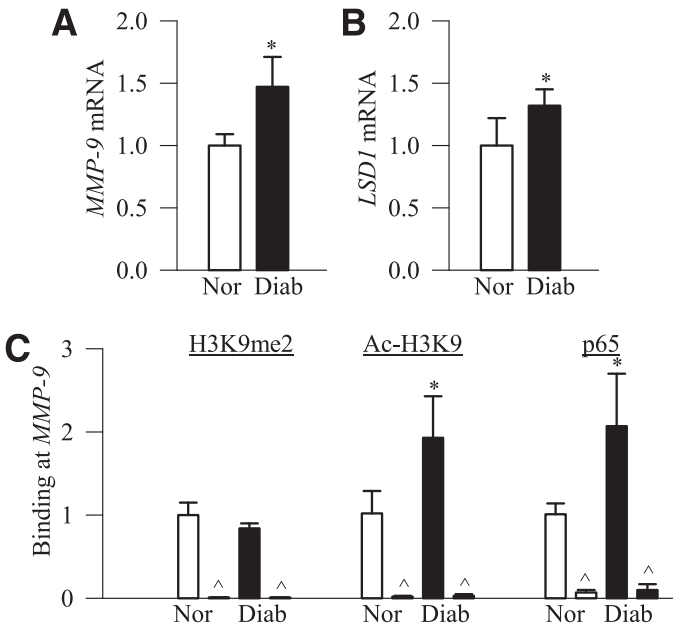

FIG. 7. Retinal MMP-9 is epigenetically modified in human donors with diabetic retinopathy. Retina from human donors with clinically documented diabetic retinopathy (Diab) and age-matched nondiabetic (Nor) donors were analyzed to quantify gene transcripts of *MMP-9* (*A*) and *LSD1* (*B*) by qPCR. *C*: Cross-linked retina was immunoprecipitated with anti-H3K9me2, acetyl (Ac)-H3K9, p65, or normal rabbit IgG, and the *MMP-9* promoter region was amplified in the precipitated DNA by SYBR green–based qPCR. IgG served as a negative antibody control (indicated as ^), and Ct values were normalized with the values from input by ddCt method. Values from the retina of nondiabetic donors are adjusted to 1 and are represented as mean ± SD from four to six samples in each group. *$P < 0.05$, compared with the values in the retina from nondiabetic donors.

NF-κB, resulting in its glucose-induced persistent activation in aortic endothelial cells (14). Furthermore, we have also demonstrated alterations in retinal global histone acetylation in diabetes and epigenetic modification of *Sod2* with increased binding of acetyl H3K9 and p65 at its promoter and enhancer (24,42).

The demethylation reaction catalyzed by LSD1 is via a redox process that produces H_2O_2 and also results in local DNA oxidation producing 8-oxo-2′-deoxyguanosine (8-OHdG) (43), and in the development of diabetic retinopathy, H_2O_2 and 8-OHdG levels are elevated in the retina and its capillary cells (25,44). In addition, MMP-9 is a redox-sensitive enzyme, which is also activated by increased oxidative stress (32), and the activated MMP-9 damages mitochondria, accelerating the apoptosis of retinal capillary cells (5,6,10). Our results clearly show that the regulation of mitochondrial superoxide prevents diabetes-induced activation of both LSD1 and MMP-9, and silencing of *LSD1* ameliorates glucose-induced mitochondrial damage (as evidenced by a decrease in the swelling and protection from partial cristiolysis), increase in ROS levels, and accelerated cell apoptosis. Thus, these results further strengthen a close association between LSD1-mediated alterations in histone methylation at the *MMP-9* promoter and mitochondrial damage in the development of diabetic retinopathy.

We have shown increased MMP-9 (activity and mRNA) in the retina and its microvessels from human donors with diabetic retinopathy (5,6), and here we show that *MMP-9* is epigentically modified with decreased H3K9me2 and increased binding of p65 at its promoter. In addition, these donors have increased *LSD1* compared with their age-matched nondiabetic donors. These results are consistent with the results from the retina of diabetic rats and retinal endothelial cells exposed to high glucose and further confirm the role of epigenetic modifications of the *MMP-9* promoter in the development of diabetic retinopathy.

The current study is focused on the regulation of MMP-9 by epigenetic modifications; however, MMP-9 activity is also regulated by TIMP-1, the tissue inhibitor selective for MMP-9, and diabetes decreases retinal TIMP-1 levels (10). Thus, the regulation of MMP-9 in diabetes by TIMP-1 cannot be ruled out. Furthermore, as mentioned earlier, diabetes also alters other MMPs, especially MMP-2, and activated MMP-2 damages mitochondria and increases pericyte death (4,7–9,45). We cannot rule out the possibility that a similar mechanism could be regulating retinal *MMP-2* in diabetes

In conclusion, we provide a novel mechanism of MMP-9 activation in diabetes; the results imply that the activated LSD1 in diabetes hypomethylates H3K9 at the *MMP-9* promoter and this frees up that lysine (K9) for acetylation. Acetyl H3K9 opens up the chromatin, increasing the accessibility to recruit the transcriptional factor NF-κB, and this culminates in the activation of MMP-9 and mitochondrial damage. Thus, the regulation of LSD1 by molecular or pharmacological means could have the potential to prevent/retard the development and progression of retinopathy by regulating MMP-9–mediated mitochondrial damage and accelerated capillary cell apoptosis in diabetic patients. Fortunately, LSD1 inhibitors have shown promising results for other chronic diseases, such as carcinoma and leukemia (46,47), and our results could support their potential benefit for diabetic retinopathy.

ACKNOWLEDGMENTS

This study was supported in part by grants from the National Institutes of Health, the Juvenile Diabetes Research Foundation, the Thomas Foundation, and Research to Prevent Blindness.

No potential conflicts of interest relevant to this article were reported.

Q.Z. planned the experiments, performed the literature search, researched data, and wrote the draft of the manuscript. R.A.K. planned the experiments, performed the literature search, and wrote and edited the manuscript. R.A.K. is the guarantor of this work and, as such, had full access to all the data in the study and takes responsibility for the integrity of the data and the accuracy of the data analysis.

The authors thank Doug Putt (Wayne State University) for technical assistance.

samples per group. Arrows indicate the mitochondria, and the bars represent 500 nm. *F*: ROS levels were quantified fluorometrically using DCDHF. 5 and 20, cells incubated in 5 or 20 mmol/L glucose for 4 days; L-si, P-si, and C, cells transfected with LSD1-siRNA, p65-siRNA, or scramble RNA, respectively, and incubated in 20 mmol/L glucose. Values obtained from untransfected control cells that were incubated in 5 mmol/L glucose are considered as 1 or 100%. *$P < 0.05$, compared with 5 mmol/L glucose; #$P < 0.05$, compared with 20 mmol/L glucose.

REFERENCES

1. Kowluru RA, Abbas SN. Diabetes-induced mitochondrial dysfunction in the retina. Invest Ophthalmol Vis Sci 2003;44:5327–5334
2. Kanwar M, Chan PS, Kern TS, Kowluru RA. Oxidative damage in the retinal mitochondria of diabetic mice: possible protection by superoxide dismutase. Invest Ophthalmol Vis Sci 2007;48:3805–3811
3. Santos JM, Tewari S, Goldberg AFX, Kowluru RA. Mitochondrial biogenesis and the development of diabetic retinopathy. Free Radic Biol Med 2011;51:1849–1860
4. Salzmann J, Limb GA, Khaw PT, et al. Matrix metalloproteinases and their natural inhibitors in fibrovascular membranes of proliferative diabetic retinopathy. Br J Ophthalmol 2000;84:1091–1096
5. Kowluru RA, Mohammad G, dos Santos JM, Zhong Q. Abrogation of MMP-9 gene protects against the development of retinopathy in diabetic mice by preventing mitochondrial damage. Diabetes 2011;60:3023–3033
6. Mohammad G, Kowluru RA. Diabetic retinopathy and signaling mechanism for activation of matrix metalloproteinase-9. J Cell Physiol 2012;227: 1052–1061
7. Mohammad G, Kowluru RA. Matrix metalloproteinase-2 in the development of diabetic retinopathy and mitochondrial dysfunction. Lab Invest 2010;90: 1365–1372
8. Mohammad G, Kowluru RA. Novel role of mitochondrial matrix metalloproteinase-2 in the development of diabetic retinopathy. Invest Ophthalmol Vis Sci 2011;52:3832–3841
9. Giebel SJ, Menicucci G, McGuire PG, Das A. Matrix metalloproteinases in early diabetic retinopathy and their role in alteration of the blood-retinal barrier. Lab Invest 2005;85:597–607
10. Kowluru RA. Role of matrix metalloproteinase-9 in the development of diabetic retinopathy and its regulation by H-Ras. Invest Ophthalmol Vis Sci 2010;51:4320–4326
11. Delcuve GP, Rastegar M, Davie JR. Epigenetic control. J Cell Physiol 2009; 219:243–250
12. Yan C, Wang H, Toh Y, Boyd DD. Repression of 92-kDa type IV collagenase expression by MTA1 is mediated through direct interactions with the promoter via a mechanism, which is both dependent on and independent of histone deacetylation. J Biol Chem 2003;278:2309–2316
13. Qin L, Han YP. Epigenetic repression of matrix metalloproteinases in myofibroblastic hepatic stellate cells through histone deacetylases 4: implication in tissue fibrosis. Am J Pathol 2010;177:1915–1928
14. Brasacchio D, Okabe J, Tikellis C, et al. Hyperglycemia induces a dynamic cooperativity of histone methylase and demethylase enzymes associated with gene-activating epigenetic marks that coexist on the lysine tail. Diabetes 2009;58:1229–1236
15. Metzger E, Wissmann M, Yin N, et al. LSD1 demethylates repressive histone marks to promote androgen-receptor-dependent transcription. Nature 2005;437:436–439
16. Liang Y, Vogel JL, Narayanan A, Peng H, Kristie TM. Inhibition of the histone demethylase LSD1 blocks alpha-herpesvirus lytic replication and reactivation from latency. Nat Med 2009;15:1312–1317
17. Hou H, Yu H. Structural insights into histone lysine demethylation. Curr Opin Struct Biol 2010;20:739–748
18. Sato H, Kita M, Seiki M. v-Src activates the expression of 92-kDa type IV collagenase gene through the AP-1 site and the GT box homologous to retinoblastoma control elements. A mechanism regulating gene expression independent of that by inflammatory cytokines. J Biol Chem 1993;268: 23460–23468
19. Ma Z, Shah RC, Chang MJ, Benveniste EN. Coordination of cell signaling, chromatin remodeling, histone modifications, and regulator recruitment in human matrix metalloproteinase 9 gene transcription. Mol Cell Biol 2004; 24:5496–5509
20. Nakamaru Y, Vuppusetty C, Wada H, et al. A protein deacetylase SIRT1 is a negative regulator of metalloproteinase-9. FASEB J 2009;23:2810–2819
21. Robert I, Aussems M, Keutgens A, et al. Matrix metalloproteinase-9 gene induction by a truncated oncogenic NF-kappaB2 protein involves the recruitment of MLL1 and MLL2 H3K4 histone methyltransferase complexes. Oncogene 2009;28:1626–1638
22. Romeo G, Liu WH, Asnaghi V, Kern TS, Lorenzi M. Activation of nuclear factor-kappaB induced by diabetes and high glucose regulates a proapoptotic program in retinal pericytes. Diabetes 2002;51:2241–2248
23. Kowluru RA, Koppolu P, Chakrabarti S, Chen S. Diabetes-induced activation of nuclear transcriptional factor in the retina, and its inhibition by antioxidants. Free Radic Res 2003;37:1169–1180
24. Zhong Q, Kowluru RA. Epigenetic changes in mitochondrial superoxide dismutase in the retina and the development of diabetic retinopathy. Diabetes 2011;60:1304–1313
25. Tewari S, Santos JM, Kowluru RA. Damaged mitochondrial DNA replication system and the development of diabetic retinopathy. Antioxid Redox Signal 2012;17:492–504
26. Ho YS, Vincent R, Dey MS, Slot JW, Crapo JD. Transgenic models for the study of lung antioxidant defense: enhanced manganese-containing superoxide dismutase activity gives partial protection to B6C3 hybrid mice exposed to hyperoxia. Am J Respir Cell Mol Biol 1998;18:538–547
27. Schramm M, Falkai P, Tepest R, et al. Stability of RNA transcripts in postmortem psychiatric brains. J Neural Transm 1999;106:329–335
28. Gutala RV, Reddy PH. The use of real-time PCR analysis in a gene expression study of Alzheimer's disease post-mortem brains. J Neurosci Methods 2004;132:101–107
29. Kowluru RA, Kowluru A, Chakrabarti S, Khan Z. Potential contributory role of H-Ras, a small G-protein, in the development of retinopathy in diabetic rats. Diabetes 2004;53:775–783
30. Syed I, Kyathanahalli CN, Jayaram B, et al. Increased phagocyte-like NADPH oxidase and reactive oxygen species generation in type 2 diabetic ZDF rat and human islets: role of Rac1-JNK1/2 signaling pathway in mitochondrial dysregulation in the diabetic islet. Diabetes 2011;60:2843–2852
31. Santos JM, Tewari S, Kowluru RA. A compensatory mechanism protects retinal mitochondria from initial insult in diabetic retinopathy. Free Radic Biol Med 2012;53:1729–1737
32. Uemura S, Matsushita H, Li W, et al. Diabetes mellitus enhances vascular matrix metalloproteinase activity: role of oxidative stress. Circ Res 2001; 88:1291–1298
33. Grant MB, Caballero S, Tarnuzzer RW, et al. Matrix metalloproteinase expression in human retinal microvascular cells. Diabetes 1998;47:1311–1317
34. Ishizaki E, Takai S, Ueki M, et al. Correlation between angiotensin-converting enzyme, vascular endothelial growth factor, and matrix metalloproteinase-9 in the vitreous of eyes with diabetic retinopathy. Am J Ophthalmol 2006;141: 129–134
35. Varier RA, Timmers HT. Histone lysine methylation and demethylation pathways in cancer. Biochim Biophys Acta 2011;1815:75–89
36. Forneris F, Binda C, Battaglioli E, Mattevi A. LSD1: oxidative chemistry for multifaceted functions in chromatin regulation. Trends Biochem Sci 2008; 33:181–189
37. Marmorstein R, Trievel RC. Histone modifying enzymes: structures, mechanisms, and specificities. Biochim Biophys Acta 2009;1789:58–68
38. Yan C, Boyd DD. Regulation of matrix metalloproteinase gene expression. J Cell Physiol 2007;211:19–26
39. Zhao X, Benveniste EN. Transcriptional activation of human matrix metalloproteinase-9 gene expression by multiple co-activators. J Mol Biol 2008;383:945–956
40. Farina AR, Cappabianca L, DeSantis G, et al. Thioredoxin stimulates MMP-9 expression, de-regulates the MMP-9/TIMP-1 equilibrium and promotes MMP-9 dependent invasion in human MDA-MB-231 breast cancer cells. FEBS Lett 2011;585:3328–3336
41. Falbo KB, Shen X. Histone modifications during DNA replication. Mol Cells 2009;28:149–154
42. Zhong Q, Kowluru RA. Role of histone acetylation in the development of diabetic retinopathy and the metabolic memory phenomenon. J Cell Biochem 2010;110:1306–1313
43. Amente S, Bertoni A, Morano A, Lania L, Avvedimento EV, Majello B. LSD1-mediated demethylation of histone H3 lysine 4 triggers Myc-induced transcription. Oncogene 2010;29:3691–3702
44. Kowluru RA, Odenbach S. Effect of long-term administration of alpha-lipoic acid on retinal capillary cell death and the development of retinopathy in diabetic rats. Diabetes 2004;53:3233–3238
45. Yang R, Liu H, Williams I, Chaqour B. Matrix metalloproteinase-2 expression and apoptogenic activity in retinal pericytes: implications in diabetic retinopathy. Ann N Y Acad Sci 2007;1103:196–201
46. Zhu Q, Huang Y, Marton LJ, Woster PM, Davidson NE, Casero RA Jr. Polyamine analogs modulate gene expression by inhibiting lysine-specific demethylase 1 (LSD1) and altering chromatin structure in human breast cancer cells. Amino Acids 2012;42:887–898
47. Schenk T, Chen WC, Göllner S, et al. Inhibition of the LSD1 (KDM1A) demethylase reactivates the all-trans-retinoic acid differentiation pathway in acute myeloid leukemia. Nat Med 2012;18:605–611